Materials analysis and particle probe: A compact diagnostic system for *in situ* analysis of plasma-facing components (invited)[a)]

C. N. Taylor,[1] B. Heim,[1] S. Gonderman,[1] J. P. Allain,[1,b)] Z. Yang,[1] R. Kaita,[2] A. L. Roquemore,[2] C. H. Skinner,[2] and R. A. Ellis[2]
[1]*School of Nuclear Engineering, Purdue University, West Lafayette, Indiana 47907, USA*
[2]*Princeton Plasma Physics Laboratory, Princeton, New Jersey 08543, USA*

(Presented 8 May 2012; received 7 May 2012; accepted 27 May 2012; published online 20 June 2012)

The objective of the materials analysis particle probe (MAPP) in NSTX is to enable prompt and direct analysis of plasma-facing components exposed to plasma discharges. MAPP allows multiple samples to be introduced to the level of the plasma-facing surface without breaking vacuum and analyzed using X-ray photoelectron spectroscopy (XPS), ion-scattering and direct recoil spectroscopy, and thermal desorption spectroscopy (TDS) immediately following the plasma discharge. MAPP is designed to operate as a diagnostic within the ~12 min NSTX minimum between-shot time window to reveal fundamental plasma-surface interactions. Initial calibration demonstrates MAPP's XPS and TDS capabilities. © *2012 American Institute of Physics*. [http://dx.doi.org/10.1063/1.4729262]

I. INTRODUCTION

Managing plasma-wall interactions in fusion devices is essential for maintaining favorable core plasma performance. Fuel recycling and erosion introduce "cold" particles into the plasma edge resulting in increased edge density, high-Z impurities, and ultimately a loss in confinement. The plasma-wall interactions can also have adverse effects on the walls. Codeposition and fuel retention, without an adequate release mechanism, would accumulate unacceptable amounts of tritium in the walls and limit usable fuel inventory. Despite the importance of the plasma-surface interface, understanding of the fundamental mechanisms has been limited due to a lack of available fusion device diagnostics capable of interrogating this region. More importantly, an understanding of the complex coupling between the core plasma and its interface with the wall is also limited by the paucity of diagnostics of plasma-facing surfaces either during or in-between shots. Furthermore, since fusion devices typically employ a limited selection of wall materials (e.g., C, W, Be, Mo, etc.), testing and diagnosing alternative materials in an operating fusion device creates a significant technical investment with potential risks.

The materials analysis particle probe (MAPP) (Ref. 1) is designed to meet the challenging physical, temporal, and technological constraints for exposure and prompt in-between-shot analysis of plasma-facing components (PFCs) exposed to plasma discharges in the National Spherical Torus Experiment-Upgrade (NSTX-U). MAPP's analysis capabilities include X-ray photoelectron spectroscopy (XPS), ion scattering spectroscopy (ISS), direct recoil spectroscopy (DRS), and thermal desorption spectroscopy (TDS). Surface chemistry is interrogated at the near surface by XPS (~8 nm probing depth), and in addition, the top 1–2 monolayers are probed using ISS. Direct recoil spectroscopy is a variation of ion scattering spectroscopy and is uniquely capable of directly detecting surface hydrogen. Heating the sample for TDS yields information on chemical binding mechanisms of deuterium retention. With incident particle energy distributions (e.g., from D ions) ranging from 5 eV up to 100's of eV, the penetration range averages on order between 1 and 100 nm (ignoring any further bulk diffusion). Therefore, this suite of diagnostics is able to capture the chemical interactions that occur at the plasma-surface interface region.

Surface chemistry analyses have been found to be useful in understanding the fundamental mechanisms responsible for plasma-surface interactions such as erosion, wall conditioning methods, and deuterium retention.[2–7] However, these offline experiments have not been able to easily analyze tokamak wall samples without *en route* air exposure, thus complicating experiments investigating hydrogen retention and analysis of reactive samples (e.g., with lithium conditioning).[7]

A more important gap is the inability to diagnose the plasma-facing surface between plasma shots to enable the correlation of surface chemistry evolution with plasma behavior. A limited number of analysis probes have been used in fusion devices to expose samples to plasma discharges and retract without breaking vacuum. The SAP (surface analysis station) operated in PLT (Princeton Large Torus) during the 1970s.[8] A tape-loop circulated from the plasma edge into an adjoined chamber 320 cm away where Auger electron spectroscopy (AES), secondary ion mass spectroscopy (SIMS), and electron stimulated desorption (ESD) were conducted. During the same time period, a linear probe in PULSATOR I inserted a sample to the plasma edge and retracted it for prompt AES, SIMS, ESD, scanning electron microscopy, and Rutherford ion backscattering analyses.[9] In DIII-D, the divertor materials evaluation system (DiMES) allowed samples to be inserted to the level of the lower divertor without breaking vessel vacuum.[10] The samples were then exchanged overnight and subsequently analyzed *ex situ* using various techniques. Another recent analysis

[a)]Invited paper, published as part of the Proceedings of the 19th Topical Conference on High-Temperature Plasma Diagnostics, Monterey, California, May 2012.

[b)]Author to whom correspondence should be addressed. Electronic mail: allain@purdue.edu.

probe was inserted in a plasma-material interface (PMI) station known as the divertor science facility,[11] and used for the study of plasma-surface interactions in the context of dust generation and transport in MAST. A PMI probe, and predecessor of MAPP, was previously installed on NSTX.[12] This allowed for sample to be exposed to plasma discharges and retracted *in vacuo*; however, *in situ* diagnostics included only TDS.

Characteristics of each of these surface analysis probes are found in the MAPP design. MAPP is part of a four-part endeavor, along with post-mortem tile analysis,[7] atomistic simulations,[13,14] and controlled laboratory experiments,[5,6,15] that aims to decipher the fundamental physics and chemistry occurring at the plasma-facing surface. The present work discusses MAPP's calibration with laboratory experiments at Purdue University. Section II of this paper describes the MAPP experiment, a detailed description of its mechanical systems, and MAPP–NSTX interface systems. Section III discusses the underlying physics of the MAPP diagnostics. Initial calibration results and discussion are presented in Sec. IV.

II. MAPP EXPERIMENT

A. Integration in NSTX

The MAPP apparatus is designed around the complex NSTX environment, with the overarching goal of providing surface characterization of samples in between plasma discharges. During the between-shot interval, shot data are acquired, wall-conditioning sequences are applied (e.g., routinely 10 min lithium evaporation[16]), and devices are prepared for the next discharge. MAPP is designed to be able to analyze samples during this 10–12 min time window without hampering other NSTX operations or other diagnostics.

MAPP is mounted to a lower dome port of NSTX using a 22°-angled 6 in CF flange. This angle is necessary to allow the MAPP probe to access an opening in the lower divertor tiles as illustrated in Fig. 1(a). When flush with the divertor tiles, the probe is positioned at a major radius of R = 0.97 m. Numerous physical and software interlocks are employed to prevent inadvertent operation of MAPP diagnostics during NSTX operation, accidental pressurization, and maintain safety. The MAPP chamber is isolated from the NSTX vessel by two actuated gate valves in series. Software interlocks require MAPP chamber pressure to be better than 5×10^{-7} Torr and the probe to be retracted prior to opening/closing NSTX valves.

NSTX operated with pulsed high magnetic fields (0.6 T) (Ref. 17) and NSTX-U will operate stronger fields near ~1 T.[18] Following a pulse, the fields decay quickly, yet result in higher ambient magnetic fields (~10 G). The MAPP analyzer (discussed in Sec. II C) detects the kinetic energy of electrons and ions; therefore, subjection to magnetic fields could attenuate the charged particles and alter collected spectra. The MAPP analyzer has been operated in laboratory-produced 16 G magnetic fields with no observed effects on collected data.

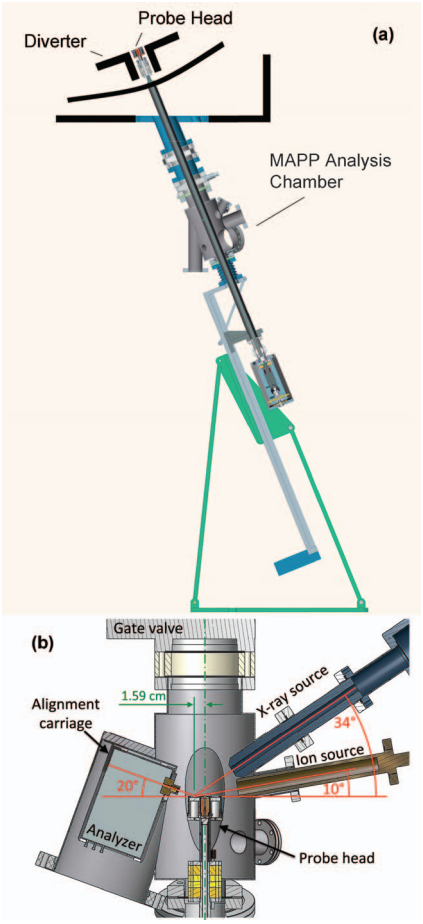

FIG. 1. (a) The MAPP chamber connects to NSTX at 22° from horizontal in order for the probe head to be flush with the lower outer divertor. (b) Sample supercenter is located 1.59 cm away from the cylindrical chamber center. The analyzer, X-ray source, and ion source point towards sample supercenter.

B. Mechanical system

1. Chamber and sample

The MAPP chamber is designed to accommodate its various diagnostics while conforming to the spatial constraints of other NSTX equipment. As a result, a custom designed compact chamber was built that includes 13 ports for analysis equipment, interfacing with NSTX, and auxiliary systems. A section view of the MAPP chamber is shown in Fig. 1(b).

Designing the port geometry required optimizing several factors. First, all diagnostics are required to be housed in one quadrant (top-front) of the MAPP chamber for two reasons; the samples cannot be inverted to view the lower two quadrants, and the top-back quadrant is inaccessible due to NSTX support structure. Second, intensities and spatially resolved information from spectroscopic techniques are optimized at specific scatter angles. In order to fit these diagnostics into the space available, the X-ray source and ion source were located in the same plane to forward-scatter towards the analyzer. The final design consideration for port placement was to choose the relative scattering angle between the excitation source, sample, and analyzer. In order to maintain consistency between MAPP and the calibration facility, Particle and Radiation Interaction with Hard and Soft

Matter (PRIHSM) (discussed later in Sec. II F), the analyzer port is angled 10° above the chamber horizontal and the X-ray source and ion source likewise have port angles of 34° and 10°, respectively. This configuration results in a scatter angle of 54° for XPS and 30° for ISS.

For analysis, the sample surface is positioned at the midplane of the 25.4-cm-long cylindrical chamber. The ports for X-ray source, ion source, residual gas analyzer, and the analyzer do not point towards the chamber supercenter (i.e., the intersection of the midplane and the cylinder axis); instead they focus on a point 1.59 cm away from supercenter. Since samples are positioned at this location for analysis, this point is identified as "sample supercenter." The chamber has additional ports designated for residual gas analysis, an optical camera, sample retrieval, pumping, and other auxiliary services.

MAPP achieves an ultimate pressure of $\sim 10^{-7}$ Torr through the use of a mechanical and ion pumps. The mechanical pumping system consists of a scroll pump and turbomolecular pump that have built-in active interlock valves to avoid back-stream pressure flow in the case of loss of pumping. Due to the high magnetic fields in the vicinity of MAPP, it is necessary to keep the rotating mechanical pumps far removed from the MAPP chamber through a ~10 foot flex hose. A 200 L/s gamma vacuum ion pump is also used to maintain vacuum. Although the ion pump has no moving parts, its large permanent magnet could generate ~5 kN · m forces if the ion pump were mounted directly onto the MAPP chamber,[19] and consequently perturb NSTX magnetic fields. To reduce these forces and magnetic field perturbation, the ion pump is mounted to the NSTX test cell floor and is connected to MAPP with ~1.2 m of tubing and flex hose. Ion pumping begins once the chamber pressure is less than $\sim 10^{-5}$ Torr. The chamber is routinely degassed using external heating strips.

The MAPP chamber has two main sections. In order to position the analyzer closest to the samples, the analyzer "chamber" was cut and welded into the primary MAPP chamber. A carriage system (Fig. 1(a)) was designed and integrated into the analyzer chamber to ensure proper analyzer alignment upon installation. The analyzer will be discussed in further detail in Sec. II C.

2. Probe and probe head

The sample probe head is illustrated in Fig. 2, and is capable of exposing four independent samples simultaneously to a plasma discharge. Samples are retained in four sample "stems" that are mounted to the probe head base. ATJ graphite samples are machined with a recessed edge to allow the sample surface to be at the same level as top of the probe stem. This avoids plasma shadowing from the sample holder support structure and also prevents the support structure from sputtering onto the sample surface. Other samples, including porous molybdenum blocks and cleaved palladium-film wafers, are mounted on support shims to provide adequate surface height for optimal plasma exposure. Beneath each sample is an independently controlled HeatWave button heater capable of heating in excess of 1000 °C. Vertical baffles deter cross-sample heating via radiation, and perforated sample stems reduce conductive heat transfer to the probe head base.

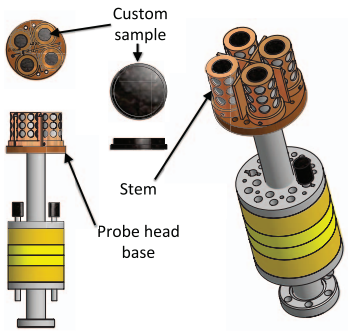

FIG. 2. Four sample stems attach to the MAPP probe head, thus being able to expose up to four samples to plasma discharges.

The probe head is attached to a linear probe that allows for 1.02 m linear motion. Three programmed set points position the sample surface at the level of the lower outer divertor plasma-facing surface, the chamber midplane for analysis, and for sample removal. A rotary drive is attached to the base of the probe to provide sample rotation. The rotary drive uses an 8-position Geneva gear that ensures that the four samples can be quickly and accurately positioned at "sample supercenter" for analysis. The remaining 4 positions on the Geneva gear are for calibration purposes.

The effect of plasma discharges on the MAPP probe presents a concern in this design. For example, halo currents through the probe can generate significant forces on the probe itself. If the probe head protrudes beyond the surface of the divertor tiles several inches, a severe halo current into the probe could be as high as 1.5 kA, which would produce an impulse of 150 N · s (the equivalent of a 10 kg mass dropped from 10 m).[19] However, positioning the probe flush with the tile surface reduces the impulse significantly to an acceptable level of 1.5 N · s (i.e., 1 kg mass dropped from 0.1 m).

C. Analyzer

A 160° hemispherical energy sector Comstock[20] analyzer is used for particle detection. The analyzer is contained within a high magnetically permeable Mu metal enclosure designed to shield low frequency magnetic fields.[21] A system of custom built power supplies and controllers is used to supply the scanning voltages needed to allow a spectrum of particle energies to pass to the detector. The analyzed electrons and ions are detected with a multi-channel plate, setup in a chevron configuration.

For XPS wide energy range scans, a 50 eV pass voltage is typically used with a 0.1 s dwell time and a 0.5 eV step. The spectrum energy range is altered depending on the sample being analyzed. For example, ATJ graphite has two prominent photoelectron peaks corresponding to O 1s (532 eV) and C 1s (284.5 eV) bonds, thus a wide-scan range up to 600 eV suffices. High-resolution region scans use a 0.05 eV step size, 0.8 s dwell time over a 10–20 eV range. ISS and DRS require that the analyzer operates with negatively charged electrostatic lenses to allow the ions to pass through to the detector. ISS and DRS spectra span the energy range equivalent to

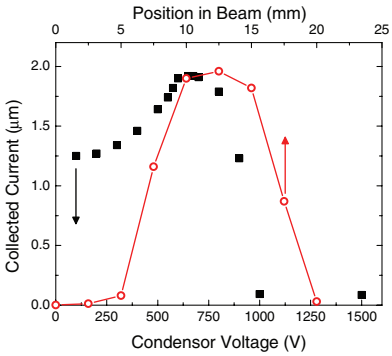

FIG. 3. Comparison of the collected current as a function of condenser lens voltage. Adjusting the condenser lens voltage focuses the ion beam spot size and the collected current. Beam current is optimized at a condenser voltage of ~675 V. At this potential, the ion beam has a FWHM of 10.0 mm.

the projectile energy (~1.5–3 keV) with a 1 eV step and a dwell time of 0.1 s per step.

The analyzer power supplies and controllers have been designed to allow for analysis to occur during the typical 10–12 min time window between NSTX discharges. Using the spectroscopic parameters described above, XPS wide scans require 2 min, XPS region scans require ~2–5 min, and ISS/DRS scans require 2–5 min of acquisition time. These analyses may be performed on one sample or all samples, as desired. Therefore, MAPP can feasibly power up necessary analytical equipment, perform a wide range XPS survey, two XPS regions, ISS and DRS scans, and power down equipment during the standard shot-to-shot time window. Full remote automation of MAPP's equipment makes this possible.[1]

D. Ion and X-ray sources

An NTI 1404 focused ion source[22] is used for ion-scattering spectroscopy as well as direct recoil spectroscopy analyses. The ion source is capable of operating with noble gases as well as several other gasses including H and O, and requires a chamber pressure of 1×10^{-7} Torr to operate. The ion energy can be tuned from 5 to 3000 eV nominally achieving beam currents of up to 10 μA. For ISS, lower beam currents are used (~150 nA); however, when operating at higher gas flow, the ion source is an effective sputtering source. Ions are produced as electrons emitted from an energized filament bombard the inlet gas molecules. The ions are extracted into the optics section with a ~850 V potential and then further accelerated or decelerated to their final energy. A condenser lens is used to shape the beam to its final size. Without condenser shaping, the beam size is a function of work distance. Thus, at the 80 mm work distance used in MAPP, a 5 mm beam can be expected. In addition, beam raster can increase the effective beam diameter for wider sample coverage. Figure 3 shows a plot of collected current as a function of condenser voltage as diagnosed and calibrated for MAPP in the PRIHSM facility. The collected beam current is optimized with a condenser voltage potential of 675 V. Under these settings a beam profile was taken and found to have a full width half maximum (FWHM) of 10.0 mm.

X-rays for XPS are produced with a water-cooled, dual anode, non-monochromatic PSP vacuum technology TX400C custom compact X-ray source.[23] Electrons emitted from an energized filament bombard an anode, which subsequently produces X-ray characteristic of the anode material. Anodes include Mg (1253.6 eV) and Al (1486.6 eV). Although better resolution can be obtained using the Mg anode, in practice, the Al anode is typically preferred for experiments involving lithium and graphite (carbon) since anode "cross-talk" can cause a ghost peaks to appear. For example, the difference in X-ray energy between the two anodes is 233 eV. While using the Mg anode, a ghost peak appears −233 eV from detected peaks (i.e., from O 1s to C 1s). For graphite, a ghost peak appears at ~52 eV (233 eV less than the 284.5 eV C 1s peak), which complicates analysis being only ~4 eV from the Li 1s peak. Ghost peaks also appear when using the Al anode, however, they are shifted +233 eV, thus avoiding close proximity to the relevant peaks being analyzed in lithiated graphite. The X-ray source is mounted on a 50 mm linear retractor that positions the source to have a working distance of 25 mm and retracts the source to allow clearance for the probe head to pass through the MAPP analysis chamber.

E. Quadrupole mass spectrometer

A quadrupole mass spectrometer is used in MAPP as a residual gas analyzer (RGA) to detect particle emission species during TDS as well for monitoring vacuum impurities. The Inficon 100L RGA (Ref. 24) is mounted line-of-sight to the sample supercenter in order to avoid potential effects from wall collisions. Residual gases (100 amu maximum) that enter the RGA are ionized near the entrance and analyzed according to mass using an oscillating quadrupole RF field. The analyzed species are allowed to pass through to the detector. When no heavy hydrocarbons are expected, partial pressures are scanned up to 50 amu with a scan time of ~9 s and resolution of five points per amu. A linear temperature ramp (~1 C/s) is maintained using a feedback input Watlow temperature controller, which simplifies interpretation of the desorption spectra.

F. Calibration with PRIHSM

The primary function of MAPP is to serve as a sophisticated *in vacuo* plasma-surface diagnostic and thus commissioning of MAPP involves calibration with the PRIHSM facility at Purdue University. PRIHSM is a unique surface science facility that is capable of *in situ* sample modification and analyses. A VG Scienta R3000 hemispherical analyzer is used in XPS as well as forward- and backward-scattering ISS. The calibration of MAPP also utilizes PRIHSM's metal thermal evaporator, residual gas analyzer, focused ion source, and diagnostics for characterizing ion beams. An adjoining chamber includes sample heaters, additional ion sources, and three independently controlled magnetron sputter sources that will be used to create W, Mo, and immiscible high/low-Z film combinations to be exposed to NSTX-U plasmas via MAPP. Additional PRIHSM capabilities are contained elsewhere.[25]

III. ANALYTICAL DIAGNOSTIC TOOLS

The analytical techniques for X-ray photoelectron spectroscopy and ion scattering spectroscopy have well been established for many years. Ample details are found in the references for XPS, ISS,[26] and DRS.[26–28] A brief summary of these techniques is included here.

A. X-ray photoelectron spectroscopy

Al and Mg X-rays produced by the MAPP source penetrate 1–10 nm depending on the substrate material. The cross sections[29] at these radiation energies show that for Li, C, and O (the dominant surface species observed in NSTX tiles) the ejection of 1s core shell electrons are 1-2 orders of magnitude more likely than the other available electrons. The photoelectron kinetic energy is equal to the incident X-ray energy minus the electron binding energy and work function. The hemispherical analyzer scans through voltages to allow electrons with different energies to pass through to the detector. The binding energy is calculated and displayed as opposed to the detected kinetic energy.

B. Ion scattering and direct recoil spectroscopy

Ion scattering spectroscopy relies on binary collision theory to identify the target mass based on the energy of a scattered ion. This requires the incident ion energy, mass, and scattering angle be well known. Since scattering relies on energy transfer from the ion projectile to the target, spectral peaks have greater separation (i.e., more easily resolved) for low projectile-target mass ratios.[26] Additionally, scattering cross sections decrease as the projectile mass and energy increase.[28] For these reasons He is commonly chosen as the source gas when analyzing low-Z targets. Less than 10% of emitted ions are secondary ions, thus, the majority of signal comes from scattered ions.[30] Therefore, ISS is sensitive to the elemental composition of the top 1–2 monolayers.

Direct recoil spectroscopy is a variation of ion scattering. The same ion source can be used as in ISS. The difference is that a higher-Z projectile is chosen. Heavy projectiles, such as Ne^+, have much higher cross sections for producing recoils than light ions, such as He^+.[28] Recoil ions are detected by the analyzer. This makes DRS one of few techniques that is capable of directly detecting elemental H on a surface.

In order to avoid compromising one sample when multiple analysis techniques are desired, both ISS and DRS use low ion currents (~150 nA), and require an acquisition time of ~100 s, thus reducing sputtering and surface mixing. DRS induces more target ion damage than ISS primarily because it requires a higher mass projectile. Scattered and recoiled ion energies are analyzed much in the same way as electrons in XPS; that is, the hemispherical analyzer scanning voltages allow a spectrum of ion energies to pass around the hemisphere for detection.

C. Thermal desorption spectroscopy

Correlating the partial pressures of thermally desorbed species to the emission temperature aids in identifying multimodal binding mechanisms. Two primary assumptions need to be considered to determine the validity of TDS deuterium retention measurements: (1) no D was released in the time elapsed between the exposures of samples to the plasma and the TDS experiment, and (2) heating was sufficient to completely deplete all deuterium from the sample. MAPP's ability to perform prompt analysis helps ensure the first condition. A future upgrade for MAPP will use laser induced breakdown spectroscopy[31] to better meet the second condition. Sequentially, TDS is performed last since it modifies the sample chemistry.

In order to calculate the total released deuterium, fragments from various species need to be accounted. For deuterium, D_2, HD, CD_4, D_2O, and HDO are routinely considered. The number of particles emitted is determined by calibrating the partial pressure against a known leak rate for that species. Retention can then be determined by taking the ratio of the release deuterium (accounting for chamber specifications) to the total incident deuterium.

IV. RESULTS AND DISCUSSION

NSTX traditionally operates predominantly with carbon PFCs; therefore, the fundamental experiment for calibrating MAPP is to characterize lithium and deuterium interactions on ATJ graphite. As XPS and TDS have been most influential in recent lithiated graphite analysis, these techniques are used in these preliminary calibration data.[2,4–6] Figure 4 compares X-ray photoelectron spectra from the O 1s energy

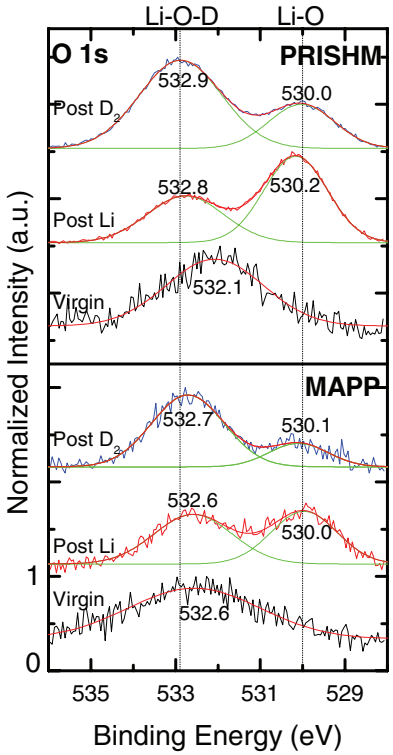

FIG. 4. The PRIHSM facility (top panel) identifies the formation of Li-O interactions at 530.0 eV (Gaussian deconvolution peak fits shown in green) in the O 1s photoelectron energy region upon lithium deposition, and Li-O-D interactions at 532.9 eV with subsequent deuterium irradiation. MAPP reproduced *post* Li and *post* D_2 peaks within 0.2 eV of the same spectra detected using the PRIHSM facility (bottom panel).

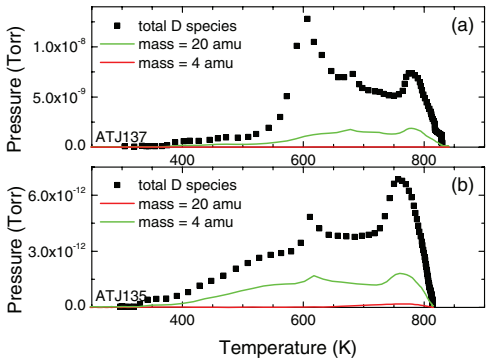

FIG. 5. Thermal desorption spectroscopy (TDS) was conducted for ATJ graphite samples exposed to (a) pre-lithium conditioned and (b) post-lithium conditioned ohmic heated NSTX plasmas. The sample with lithium conditioning released significantly more deuterium.

range collected using MAPP and the PRIHSM facility. In each case, lithium (1–2 μm) was deposited on polished yet otherwise virgin ATJ graphite, followed by deuterium irradiation (10^{16}–10^{17} cm^{-2}). Virgin graphite has a prominent peak at 532 eV. In the PRIHSM and MAPP experiments, following lithium deposition, a new peak forms at ~530 eV. The formation of this new peak indicates that lithium is chemically binding with oxygen on the sample. In Fig. 4, the difference in the relative intensities in the MAPP vs. PRIHSM Li-O peaks has been attributed to lithium dose, time after deposition, and surface morphology.[6] After deuterium irradiation of the lithiated graphite sample, the peak at 533 eV enhances, and has been previously identified as a deuterium-oxygen interaction that only occurs in the presence of lithium.[5] Similar experiments have been used previously to identify fundamental mechanisms of deuterium retention,[6,14] relate deuterium fluence to lithiated graphite saturation,[5] and characterize post-campaign NSTX tiles.[7] In MAPP, XPS capability will serve as the primary diagnostic to elucidate fundamental Li and D interactions on ATJ graphite, Mo, and porous-Mo tiles. These analyses will also provide information on the dynamic influence of successive discharges on wall samples, and the retention capacity of various samples.

MAPP takes advantage of our previous experience with thermal desorption spectroscopy from its predecessor PMI probe. Sets of four samples (primarily ATJ graphite and Pd) were exposed to NSTX discharges prior to the NSTX campaign's first lithium conditioning and following lithium conditioning.[12] One graphite sample from each exposure was heated in the PMI probe to measure the prompt desorption of deuterium-containing species with remaining samples being analyzed in greater detail at Purdue University.[12] Figure 5 shows thermal desorption spectra of two ATJ graphite samples exposed to 10 Ω heated NSTX plasma discharges, which were analyzed at Purdue (due to heating difficulties in the PMI probe). These spectra prominently display 2 peaks, indicating weakly bound deuterium near 600 K and strong covalent/ionic bound deuterium near 800 K.[12]

In summary, the MAPP will enable the direct and prompt analysis of plasma-facing components exposed to NSTX-U plasmas provided by a suite of diagnostics. XPS, ISS, DRS, and TDS will be used to determine how existing and novel PFCs respond to and are affected by NSTX-U plasma discharges. Because of MAPP's versatility, this diagnostic can be operated without interrupting NSTX-U operations.

ACKNOWLEDGMENTS

In addition to contributing as coauthor, B. Heim merits special acknowledgement for leading the MAPP effort and for the countless hours spent creating MAPP. At Purdue, we would like to acknowledge and thank M. Gonzalez for his assistance in CAD design, modeling parts of the probe, and help in assembling MAPP; E. Collins for his design of the analyze power supplies; D. L. Rokusek for determining many of the specifications needed for the analysis equipment. We also thank and acknowledge W. Blanchard, H. W. Kugel, and M.G. Bell at Princeton Plasma Physics Laboratory (PPPL) for their input on the design, safety, and integration; the many PPPL technicians, draftsmen, and engineers for their development of MAPP support structures and maintenance; M. Nieto for his help with TDS calculations. Work supported by Department of Energy (DOE) (Grant Nos. DE-FG02-09ER55015 and DE-AC02-09CH11466).

[1] B. Heim *et al.*, IEEE Trans. Plasma Sci. **40**(3), 735–739 (2012).
[2] J. P. Allain *et al.*, J. Nucl. Mater. **390**, 942–946 (2009).
[3] H. Dylla, J. Nucl. Mater. **93**, 61–74 (1980).
[4] S. S. Harilal *et al.*, Appl. Surf. Sci. **255**(20), 8539–8543 (2009).
[5] C. N. Taylor, J. P. Allain, B. Heim, P. S. Krstic, C. H. Skinner, and H. W. Kugel, J. Nucl. Mater. **415**(1), S777 (2011).
[6] C. N. Taylor *et al.*, J. Appl. Phys. **109**(5), 053306 (2011).
[7] C. N. Taylor *et al.*, "Surface chemistry analysis of lithium conditioned NSTX graphite tiles correlated to plasma performance," Nucl. Fusion (submitted).
[8] H. Dylla and S. Cohen, J. Nucl. Mater. **63**, 487–494 (1976).
[9] P. Staib and G. Staudenmaier, J. Nucl. Mater. **63**, 37–46 (1976).
[10] C. Wong *et al.*, J. Nucl. Mater. **196**, 871–875 (1992).
[11] G. De Temmerman *et al.*, Nucl. Fusion **50**, 105012 (2010).
[12] C. H. Skinner *et al.*, J. Nucl. Mater. **415**, S773–S776 (2010).
[13] P. S. Krstic, J. P. Allain, A. Allouche, J. Jakowski, J. Dadras, C. N. Taylor, and Z. Yang, Fusion Eng. Des. (in press).
[14] P. S. Krstic, J. P. Allain, C. N. Taylor, J. Dadras, S. Maeda, K. Morokuma, J. Jakowski, A. Allouche, and C. Skinner, "Tuning fusion plasma behavior at the nanoscale on lithium-based surfaces," Sci. Rep. (submitted).
[15] C. N. Taylor, J. P. Allain, P. S. Krstic, J. Dadras, R. Kaita, H. W. Kugel, and C. H. Skinner, "The role of oxygen in retaining deuterium on lithiated graphite surfaces," J. Nucl. Mater. (submitted).
[16] H. W. Kugel *et al.*, J. Nucl. Mater. **390–391**, 1000 (2009).
[17] M. Bell *et al.*, Nucl. Fusion **46**, S565 (2006).
[18] J. E. Menard *et al.*, "Overview of the physics and engineering design of NSTX Upgrade," in *2011 IEEE/NPSS 24th Symposium on Fusion Engineering (SOFE)*, 26–30 June 2011, Chicago, IL.
[19] M. G. Bell, private communication (2010).
[20] Comstock, Inc., model AC-901.
[21] D. D. L. Chung, J. Mater. Eng. Perform. **9**(3), 350–354 (2000).
[22] Nonsequitur Technologies Inc., model 1404.
[23] Tectra/PSP Vacuum Technology, model TX400C.
[24] Inficon., model 100L.
[25] O. El-Atwani, J. Allain, and S. Ortoleva, Nucl. Instrum. Methods Phys. Res. B **272**, 210–213 (2012).
[26] M. D. Coventry and R. Bastasz, Nucl. Instrum. Methods Phys. Res. B **243**(1), 193–199 (2006).
[27] J. W. Rabalais, Crit. Rev. Solid State Mater. Sci. **14**(4), 319–376 (1988).
[28] W. Eckstein, Nucl. Instrum. Methods Phys. Res. B **27**(1), 78–93 (1987).
[29] J. J. Yeh and I. Lindau, At. Data Nucl. Data Tables **32**(1), 1–155 (1985).
[30] J. P. Allain *et al.*, Rev. Sci. Instrum. **78**, 113105 (2007).
[31] B. Schweer *et al.*, Phys. Scr. **2009**, 014008 (2009).